Rhodium mediated stereoselective polymerization of carbenes

Jellema, E.

Publication date
2010

Chapter 6

Investigations into initiation, termination and chain-transfer mechanisms during Rh-mediated carbene polymerization reactions

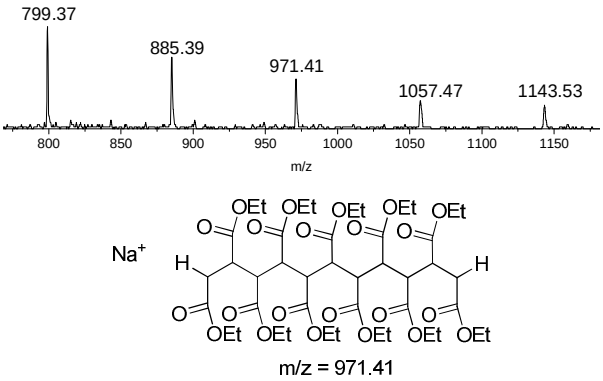

6.1 Introduction

In the previous Chapters we saw that the Rh-mediated polymerization of carbenes is a valuable method for the preparation of highly functionalized, stereoregular and high molecular weight polymers.[1] Different catalyst precursors were described for the polymerization of carbenes from diazoacetates to afford syndiotactic ester-functionalized polymethylenes with a high molecular weight (Scheme 1).[2-5]

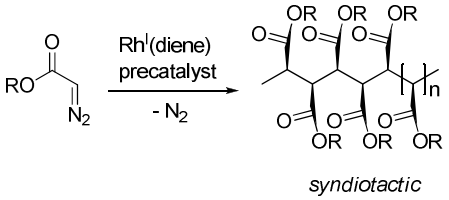

Scheme 1. Rh^{I}(diene) mediated polymerization of carbenes from diazoesters, showing syndiotactic poly(alkyl 2-ylidene-acetate).

The polymer properties can be influenced by using different ligands; molecular weights (M_w) in the range of ~150-770 kDa are possible.[3,5] In Chapter 5 an efficient catalyst precursor was introduced, leading to formation of the polymer in high yields (up to 80%).[5]

A mechanism was proposed to describe the propagation steps based on experimental and computational investigations (Chapter 4).[3] However, the initiation efficiency of the polymerization reaction is in general low and the initiation and termination processes are not well understood. In this Chapter, investigations to understand these processes are described, focusing on the influence of different (pre-activated) catalysts, additives and reaction conditions on catalyst (de)activation, initiation, termination and chain-transfer processes. Additionally, we explored the influence of the formed side products on the actual polymerization reaction.

6.2 Results and discussion

6.2.1 Exploring the reactivity of Rh-alkyl/aryl complexes in the polymerization of EDA

Ligand variation and computational studies led to a proposed mechanism for the propagation steps of the polymerization of carbenes from diazo compounds (Chapter 4). In this mechanism, a [(diene)Rh^{I}-alkyl] complex was proposed as the active species (Scheme 2).

The evaluation of Rh-alkyl complexes resembling the proposed active species as catalysts for the polymerization of carbenes can give more insight in the initiation

mechanism of the reaction. A higher initiation efficiency is expected when using Rh-alkyl compounds than the *N,O*-ligand supported analogues used in the previous Chapters (up to ~5%), since it was proposed that the active species are formed from the Rh(diene) catalyst precursors in the initial stages of the reaction with the diazo compounds.

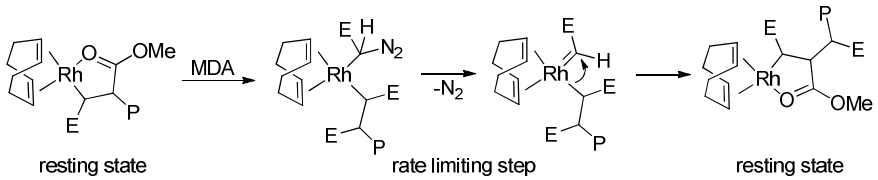

Scheme 2. Proposed mechanism of propagation steps of the Rh-mediated polymerization of polar functionalized carbenes (P = growing polymer chain, E = COOMe).

Several Rh-alkyl/aryl complexes are described in the literature. These complexes are often stabilized by sterically demanding ligands and/or additional donor ligands (*e.g.* phosphines or amines), which makes them less reactive towards substrates. A selection of such complexes was used for evaluation in the polymerization of EDA (see Scheme 3).

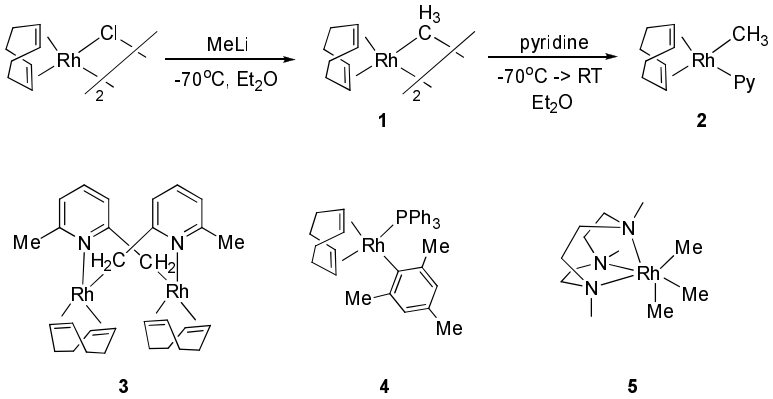

Scheme 3. Rh-alkyl/aryl complexes evaluated for the polymerization of EDA (Py = pyridine).

All compounds in Scheme 3 are described in the literature, except complex **4**. This Rh-aryl complex was synthesized from $[\{Rh^{I}(1,5\text{-cyclooctadiene})(\mu\text{-Cl})\}]_2$, triphenylphosphine and mesityl lithium in moderate yield (37%). Somewhat related complexes were reported in the literature as catalysts for the polymerization of acetylenes and isocyanides.[6] For example, with $[(Ph_2C{=}CPh)Rh^{I}(tfb)$-(triphenylphosphine)] (tfb = tetrafluorobenzobarrelene) quantitative initiation efficiency was achieved in the polymerization of phenylacetylene.[6b]

Crystals of **4** suitable for X-ray diffraction were obtained by crystallization from *n*-hexane. The molecular structure and selected bond distances and angles are depicted in Figure 1 and Table 1.

The molecular structure of **4** shows a square planar environment around rhodium with bond lengths and angles similar to related complexes in the literature.[6a,7]

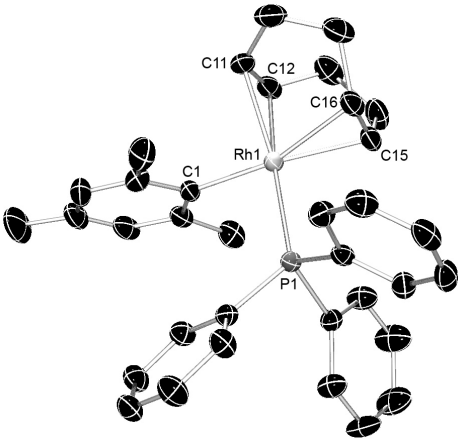

Figure 1. Molecular structure of **4** with 50% probability ellipsoids. Hydrogen atoms are omitted for clarity.

Table 1. Selected bond lengths (Å) and angles (°).

	2b
Rh(1)–P(1)	2.3153(9)
Rh(1)–C(1)	2.056 (3)
Rh(1)–C(11)	2.194(3)
Rh(1)–C(12)	2.201(3)
Rh(1)–C(15)	2.202(3)
Rh(1)–C(16)	2.253(3)
C(11)–C(12)	1.361(5)
C(15)–C(16)	1.365(5)
C(1)–Rh(1)–P(1)	90.83(8)
C(1)–Rh(1)–C(11)	86.90(13)
P(1)–Rh(1)–C(11)	160.51(10)

The Rh-alkyl/aryl complexes shown in Scheme 3 were evaluated in the polymerization of carbenes from EDA (Table 2). Complexes **3**,[8] **4** and **5**[9] are relatively air- and moisture stable and can easily be handled. These compounds were applied in a similar way as described in the previous Chapters, by addition of EDA to a solution of the complex in dichloromethane or chloroform (entries 3-6). Rh^{III}-complex **5** was activated by reaction with HBArF ($[H(OEt_2)_2]B(C_6H_3(CF_3)_2)_4$)[10] prior to addition of EDA, but was not reactive (entry 6).

Complexes **1**[11] and **2**[12] were not isolated before reaction with EDA. The thermally unstable Rh-complex **1** was prepared in Et_2O at −70°C and subsequently the reaction mixture was warmed to −40°C. EDA was added (200 equivalents) and the mixture was warmed to room temperature. For **2** this was done in a similar way, by addition of EDA after reaction of **1** with pyridine.

Table 2. Polymerization of EDA with Rh-alkyl/aryl complexes.[a]

entry	catalyst precursor	Rh:EDA	solvent	polymer yield (%)[b]	M_w (kDa)[b,c]	M_w/M_n[b,c]	IE (%)[d]
1	**1**[e,f]	1 : 200	Et_2O	3	164[g]	8.3	3
2	**2**[f,h]	1 : 100	Et_2O/DCM	6	221[g]	8.3	2
3	**3**	1 : 90	DCM	10	82	3.3	3
4	**4**	1 : 50	$CHCl_3$	41	269[g]	6.3	5
5	**4**[f]	1 : 500	$CHCl_3$	3	125	4.1	4
6	**5**[i]	1 : 100	DCM	no reaction	-	-	-

[a] Conditions: see experimental section. [b] Isolated by precipitation and washing with MeOH. [c] SEC analysis calibrated against polystyrene samples. [d] Initiation efficiency: number of polymer chains per Rh in % (mol/mol × 100%). [e] Prepared *in situ* from [{Rh^I(1,5-cyclooctadiene)(μ-Cl)}]$_2$ and MeLi. [f] Incomplete conversion. [g] Bimodal distribution. [h] Prepared *in situ* from [{Rh^I(1,5-cyclooctadiene)(μ-Cl)}]$_2$, MeLi and pyridine. [i] With addition of ~2 equivalents of HBArF.

For most test reactions a higher EDA : Rh ratio was used than usual to ensure the formation of polymers of a certain molecular weight in case of an anticipated higher initiation efficiency. The polymerization reactions with **1** and **2** afforded only low polymer yields; 3 and 6% respectively (entries 1 and 2). The size exclusion chromatograms show broad and bimodal distributions, but high molecular-weight polymers.

The yields with compounds **3** and **4** are slightly higher than with **1** and **2** and the molecular-weight distributions are narrower. Complex **4** performs better when the catalyst loading is higher; the yield improves from 3 to 41% and the EDA is completely converted in the latter case (entries 4 and 5). Overall, high molecular weight polymers are formed with these Rh-alkyl/aryl complexes.

Assuming that each chain grows from a single Rh atom and no chain-transfer occurs, the initiation efficiency (IE: the average number of chains per Rh in %) can be estimated from M_n and the yield of the polymer (Table 2).[5] This number is not higher for any of the reactions in Table 2 compared to what was described in the previous Chapters (up to ~5%). The results show that the initiation efficiency is not higher when using well-defined (diene)Rh-methyl/aryl complexes as catalyst precursors (compared to (diene)Rh complexes without alkyl/aryl ligands).

Possibly, the Rh-complexes evaluated here (**1**-**5**) are not reactive enough (and/or the reaction of **1** and **2** is hindered by side products due to the *in situ* synthesis of the catalysts), but from the results obtained thus far it seems that even the well-defined [(diene)Rh^I-alkyl] model species in Scheme 2 are still merely precatalysts instead of the true active polycarbene producing species. Catalyst activation under the applied reaction conditions seems to be important for formation of the species that produce high molecular-weight and stereoregular polymers.

6.2.2 Characterization of the oligomeric side products

Polymer end-group analysis generally provides valuable information about the initiation and termination processes of a polymerization reaction. However, the polymers described so far have high molecular weights and a broad molecular

weight distribution, which makes them unsuitable for end-group analysis by NMR spectroscopy or mass spectrometry. Hence, we resorted to analyzing the oligomeric fractions, which are generally obtained with a relatively narrow M_w distribution and have the appropriate molecular weight range for MALDI-ToF mass spectrometry analysis. These data are described in this section.

The oligomeric products are isolated from the reaction mixture by precipitation of the polymer with methanol.[3-5] The polymeric fraction is separated from the reaction mixture by filtration or centrifugation, while the oligomeric (and dimeric) products remain dissolved in the methanol. Evaporation of the solvent and subsequent prolonged drying under vacuum to remove the dimeric products (diethyl maleate and fumarate) leaves the oligomeric fraction as a dark brown viscous oil. This material shows broad signals in the ^{1}H and ^{13}C NMR spectra (see Figure 3 in Chapter 2) indicative of ill-defined, atactic (and possibly branched) oligomers.

In Chapter 4 we suggested that different active species could be responsible for the formation of the polymeric and oligomeric products. SEC-analysis of the reaction products supports this. For example, the SEC-traces of the methanol soluble and insoluble products of the reaction of EDA with pre-catalyst **6** or **7** (Figure 2), show clearly two separate signals, which do not, or hardly overlap (Figures 3 and 4).

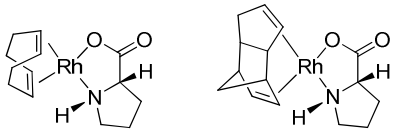

6 **7**

Figure 2. Pre-catalysts **6** and **7**.

The oligomers obtained with both **6** and **7** have similar low molecular weights in the range of 1.1 kDa, while the polymers have significantly different molecular weights. The polymers and oligomers prepared with **7** show no overlap between the two signals at all (Figure 4). The most straightforward explanation for this behavior is that the oligomeric fraction is produced by a different type of active Rh-species than those responsible for the formation of the polymeric fraction. Hence, at least two different active species are produced from the catalyst precursors under the applied catalytic conditions.

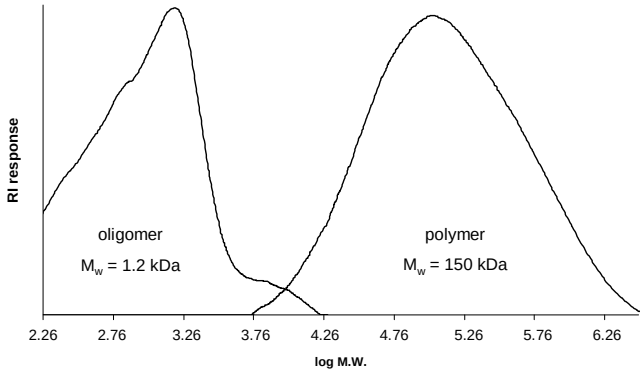

Figure 3. SEC-trace of polymeric (methanol insoluble) and oligomeric (methanol soluble) products of a reaction of **6** with EDA (the signal intensities are normalized for easier comparison).

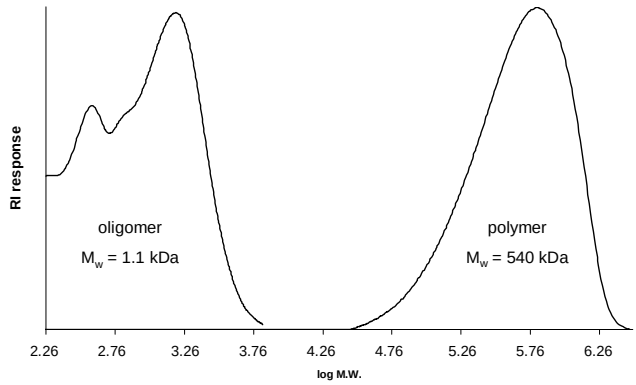

Figure 4. SEC-trace of polymeric (methanol insoluble) and oligomeric (methanol soluble) products of a reaction of **7** with EDA (the signal intensities are normalized for easier comparison).

Since the broad signals in the NMR spectra (see Figure 3 in Chapter 2) did not give detailed information about the oligomeric species, other techniques were used for their analysis. The IR spectra of polymer and the oligomers are similar (Figure 5), with the most significant differences being additional vibrations for the oligomeric species at ~1600 cm^{-1} and ~1200 cm^{-1}. The ^{1}H NMR spectrum of the oligomer sample used for IR spectroscopy is similar to Figure 3 in Chapter 2; no dimers were present in the mixture that was analyzed. Possibly, these extra signals stem from (parts of) the catalyst precursor and/or oligomer ester moieties coordinated to rhodium remains.

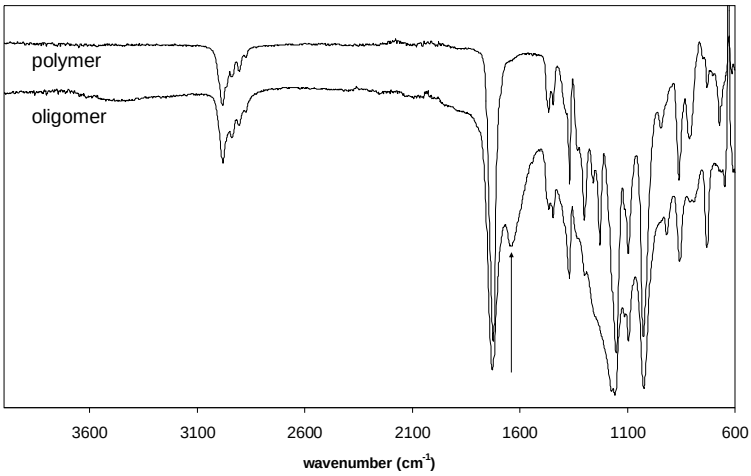

Figure 5. IR-spectrum of polymeric and oligomeric products of a reaction of **6** with EDA.

In Chapter 2 the possibility of organometallic end-groups was mentioned. In the methanol soluble fraction of the reaction mixture of **6** or **7** (Figure 2) with EDA rhodium is clearly present as is evidenced by elemental analysis (Table 3, entries 4 and 5). The amount of rhodium found in the oligomeric fraction corresponds with ~0.5-1 Rh atoms per oligomeric chain, leaving the possibility of rhodium still being attached to the oligomeric chains as one of the chain ends. From these results alone it is not clear whether the rhodium is indeed still attached and therefore we further analyzed the oligomers with MALDI-ToF mass spectrometry.

Table 3. Elemental analysis of polymer and oligomers of EDA.

entry	polymer/oligomer	precatalyst		C	H	N	Rh
1	polymer		calculated	55.81	7.02	-	-
2	polymer	**6**	found	55.67	6.91	n.d.	0.09
3	oligomer	**7**	found	51.11	6.24	1.47	n.d.
4	oligomer	**6**	found	51.22	6.36	1.19	5.46
5[a]	oligomer	**6**	found	49.77	6.26	0.81	4.50

[a] Filtrated through silica before analysis.

To gain more insight in the initiation capabilities of the σ-donor ligands bound to the applied Rh^{I}(diene) complexes, the oligomeric products of the reactions of catalyst precursors **1**, **4**, **6** and **8**-**12** (see Figure 6) with EDA were all analyzed by MALDI-ToF mass spectrometry. Some oligomer samples were purified by filtration through a silica plug before analysis (see experimental section), but this did not lead to a clear difference in the obtained spectra.

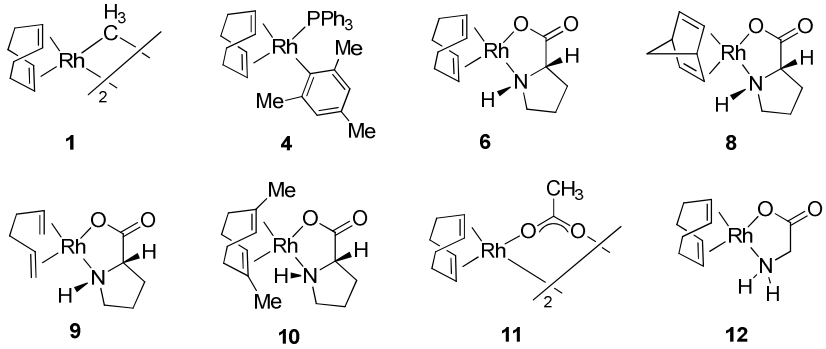

Figure 6. Catalyst precursors used for the polymerization of EDA.

In the spectra the signals with the highest intensities are found around 800 m/z, corresponding with low molecular weight polycarbene chains. The clearest picture was obtained for the oligomers obtained with [(*L*-prolinate)Rh^{I}(2,5-norbornadiene)] (**8**); one clear series of signals with a repetitive unit of 86 Da (the mass of one carbene unit: CHCOOEt) is observed in Figure 7.

The peaks correspond to $(CHCOOEt)_n$ + 25 Da (*e.g.* 779.37 Da, with n = 9), which we interpret as oligomeric chains with two hydrogen-atom chain-ends and Na^+ as a charge carrier: $[Na]^+\{(H–(CHCOOEt)_9–H)\}$. The analysis was also performed with addition of lithium trifluoroacetate, resulting in a clear series corresponding to $[Li]^+\{(H–(CHCOOEt)_n–H)\}$.

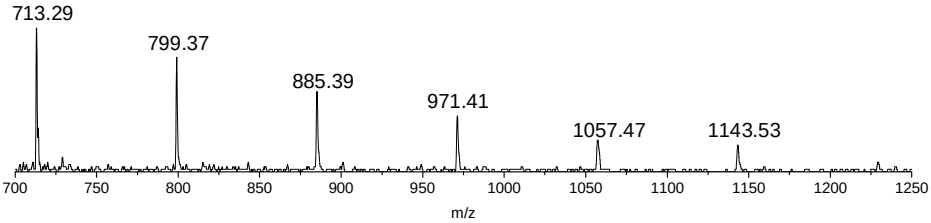

Figure 7. Part of the MALDI-ToF mass spectrum (reflectron mode) of oligomers obtained with **8**.

For most of the oligomeric samples obtained with the other catalyst precursors, masses corresponding to the same saturated species are observed: $[Na]^+\{(H–(CHCOOEt)_n–H)\}$ (Figure 8). These spectra are not as clean as the one of the oligomeric species obtained with **8**, but the peaks can be distinguished (the marked peaks). Unfortunately, we were not able to assign the other peaks.

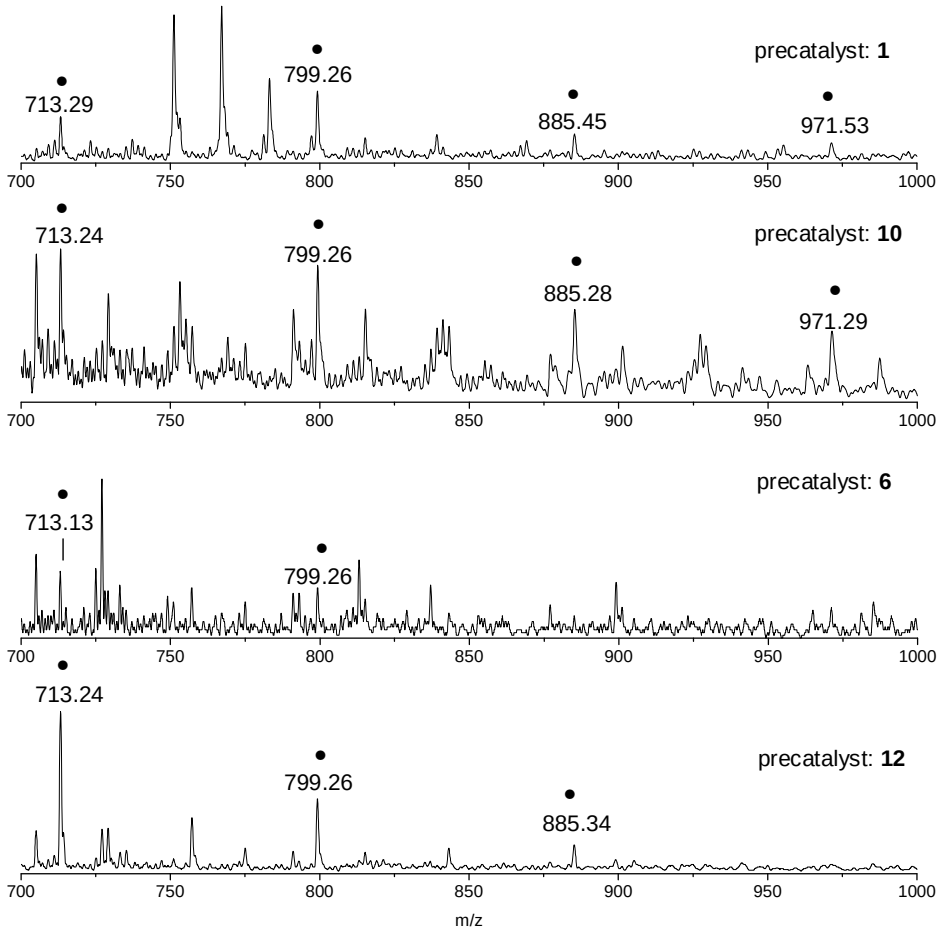

Figure 8. Part of the MALDI-ToF mass spectrum (reflectron mode) of oligomers obtained with **1**, **6**, **10** and **12**.

Addition of lithium trifluoroacetate to the oligomeric sample obtained with **12** confirmed that the signals correspond to $[Na]^+\{(H–(CHCOOEt)_n–H)\}$; the peaks marked in Figure 8 (bottom) shift by 16 Da to lower masses ($[Li]^+\{(H–(CHCOOEt)_n–H)\}$).

The spectrum of the oligomers obtained with **9** shows a large number of signals. Addition of sodium or lithium salts leads to a clearer image (Figure 9), with in both spectra two series with a repeating unit of 86 Da. The series with mass 885 (Figure 9, top) and 869 Da (Figure 9, bottom) correspond with $[Na]^+\{(H–(CHCOOEt)_n–H)\}$ and $[Li]^+\{(H–(CHCOOEt)_n–H)\}$, respectively. The other series are also fragments with sodium or lithium as charge carrier and are shifted by 44 Da to higher mass (compared to the series corresponding with $[M]^+\{(H–(CHCOOEt)_n–H)\}$), but it is not clear how this series should be interpreted in terms of chain-ends.

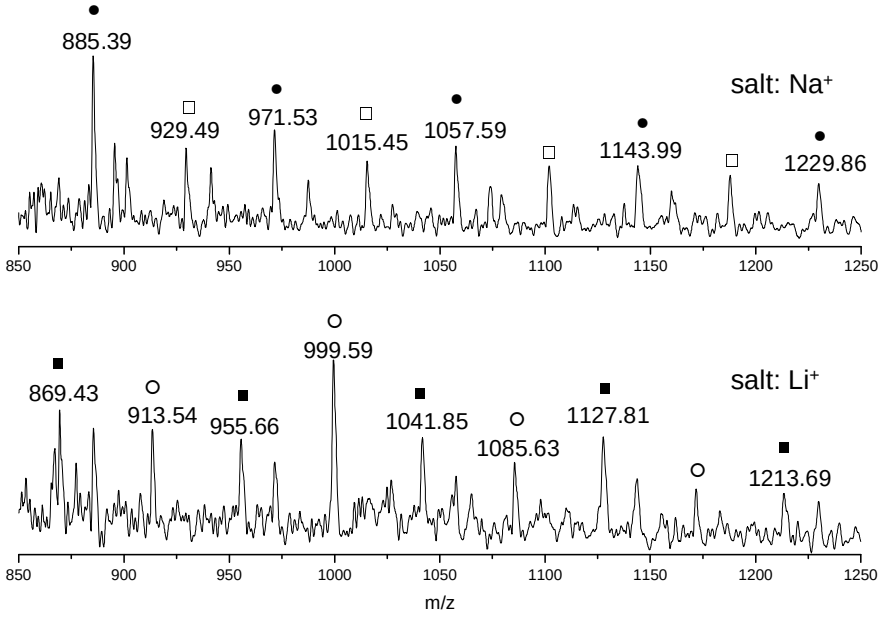

Figure 9. Part of the MALDI-ToF mass spectra (reflectron mode) of oligomers obtained with **9** (sample with top: sodium trifluoroacetate and bottom: lithium trifluoroacetate).

For catalyst precursors **4** and **11** the same series are visible as discussed for the previous spectra, corresponding to the saturated species: $[Na]^+\{(H-(CHCOOEt)_n-H)\}$ (signals with masses 713, 799, 885, *etc*. in Figure 10).

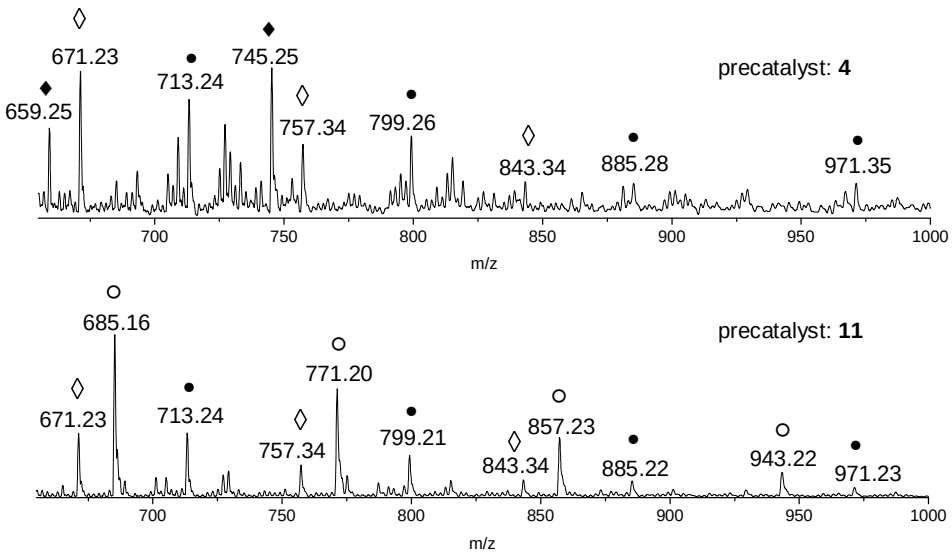

Figure 10. Part of the MALDI-ToF mass spectra (reflectron mode) of oligomers obtained with **4** and **11**.

Interestingly, two other series were observed pointing to a mesityl chain-end ($[Na]^+\{(H–(CHCOOEt)_n–Mes)\}$, masses: 659, 745, *etc.*) and an acetate chain-end ($[Na]^+\{(H–(CHCOOEt)_n–OC(Me)=O)\}$, masses: 685, 771, 857, *etc.*). Additional series with masses of 671, 757, *etc.* without the added salt ions as charge carrier could not be assigned.

The observed mesityl and acetate chain-ends stem from the complexes **4** and **11**, respectively, where they were bound as ligands to rhodium. This means that (part of) the chain-initiation must have proceeded via carbene insertion into the Rh–C or Rh–O bonds with the mesityl and acetate ligands in **4** and **11**. However, it is also clear that the repeating mass patterns of all analyzed oligomeric fractions are dominated by series of the same saturated poly-carbene fragments in the mixture: $[Na]^+\{(H–(CHCOOEt)_n–H)\}$. Most likely the latter chains started to grow from a Rh-hydride species, and must be terminated by protonation (*e.g.* by adventitious ethanol or water present in the reaction mixture or as a result of the work-up with methanol). In most of the mass spectra several peaks were observed, which could not all be identified. For these species an organometallic end-group is still a possibility.

The most straightforward explanation for the above observations is that the (diene)Rh precatalyst becomes modified under the applied catalytic reaction conditions in the beginning of the reaction with EDA (Figure 11). Most likely, the precatalysts **A** (Figure 11a) (generic formula (diene)Rh–Y, in which Y = nucleophilic donor ligand) react with the diazo compounds N_2=CHE (*e.g.* EDA) through carbene insertion into the Rh–Y bonds. We propose that with the unmodified (diene)Rh species this leads to only a few insertions (**B** in Figure 11a), followed by rapid β-H elimination to form the (diene)Rh–H species **C**. Carbene insertion into the Rh–H bond of unmodified **C** would then again lead to rapid β-H elimination, thus explaining the carbene dimerization activity in the beginning of the reaction (see Chapter 4).[3] During the first 30 minutes of the reaction it seems that the (diene)Rh species are modified under the applied catalytic reaction conditions to form a different, modified active species: (diene')Rh. The ability of these modified species (diene')Rh to undergo β-H elimination seems to be absent or be markedly suppressed compared to that of the starting (diene)Rh species, thus leading to oligomerization from the (diene')Rh–Y and (diene')Rh–H species **D** (Figure 11a) and **G** (Figure 11b), respectively. This explains the observation of both –H and –Y chain-ends from a chain-initiation perspective. The observation of –H chain-ends from a chain-termination perspective is indicative for protonolysis of the Rh–C bonds to liberate the growing chain fragments from the metal. The markedly suppressed or absent ability of the Rh-chain species to undergo β-hydrogen elimination is quite remarkable for rhodium.

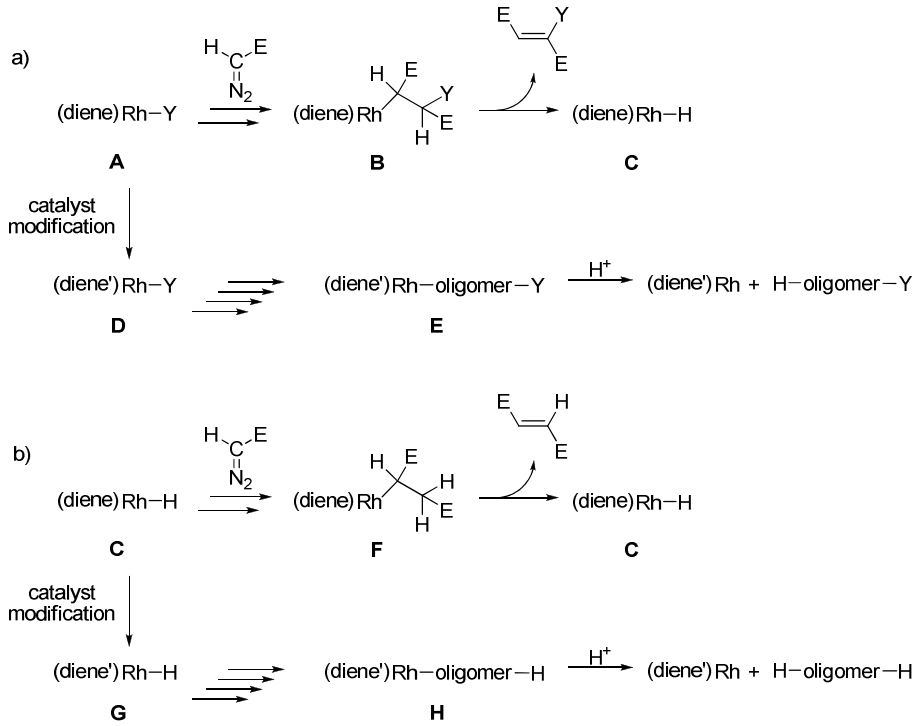

Figure 11. Proposed product formation in reaction of the Rh-catalyst precursor with EDA.

Protonolysis could be induced by traces of water or ethanol present in the reaction mixture (stabilizer in chloroform), but the protons may also stem from the workup with MeOH or even from the somewhat acidic EDA.[13] It seems that during the reaction the (diene')Rh species are further modified so that the remaining active (diene'')Rh species produce only high molecular weight and stereoregular polymers instead of short, atactic oligomers.

6.2.3 The influence of alcohols on the polymerization of EDA

In Chapter 2, analysis of polymers by MALDI-ToF mass spectrometry was described. Chains with a combination of end-groups –OH and –H as well as –H and –H were detected (see section 2.2.6). Likely, these chains were initiated by nucleophilic attack of OH^- at a metal carbene species and terminated by protonolysis, in good agreement with the above data concerning chain-end analysis of the oligomeric fractions (section 6.2.2). The possibility of improving the initiation efficiency of the polymerization reaction by addition of water and alcohols was investigated and is described in this section.

The experiments were performed with [(*L*-prolinate)Rh^I(1,5-cyclooctadiene)] (**6**) and EDA in the presence of water and different amounts of methanol (Table 4). The influence of other alcohols was also investigated (Table 5).

Table 4. Polymerization of EDA with **6** in mixtures of chloroform and methanol.[a]

entry	MeOH (mL)	$CHCl_3$ (mL)	EDA (mmol)	polymer yield (%)[b]	M_w (kDa)[b,c]	M_w/M_n[b,c]	IE (%)[d]
1	0	5	2.0	45	150	3.6	4.6
2	1	5	2.0	40	86	3.4	6.8
3	2.5	2.5	1.7	7	30	1.9	1.6
4	5	0	1.7	5	35	2.2	1.1
5	0.02 mL H_2O	5	1.8	30	165	3.7	2.8

[a] Conditions: 0.04 mmol catalyst, room temperature, reaction time: 14 hours. [b] Isolated by precipitation and washing with MeOH. [c] SEC analysis calibrated against polystyrene samples.[d] Initiation efficiency: number of polymer chains per Rh in % (mol/mol × 100%).

The addition of water has a negative effect on the polymer yield (entry 5), while the polymers have a similar M_w compared to the reaction without water (entry 1). Due to the low solubility of water in chloroform, we continued the investigation concerning the influence of protic additives using varying amounts of methanol.

Addition of 1 mL of methanol affords the polymer in similar yields (~ 40%) as in the reactions without methanol (entries 1 and 2). The polymer molecular-weights clearly decrease with increasing amounts of methanol. Addition of 2.5 mL or more methanol results in precipitation of the polymer during the reaction, which may explain in part the observed lower yields (entries 3 and 4). Interestingly, the initiation efficiency increases significantly upon addition of up to 1 mL of methanol (entries 1 and 2).

Analysis of the polymers with size-exclusion chromatography clearly shows that the molecular weight distribution of the polymers becomes narrower upon addition of methanol (Figure 12). The shift to lower mass with increasing amounts of methanol is clearly visible. The polymer synthesized in the presence of 1 mL of methanol shows a bimodal distribution consisting of a dominating signal at lower molecular weights and a shoulder at higher molecular-weights.

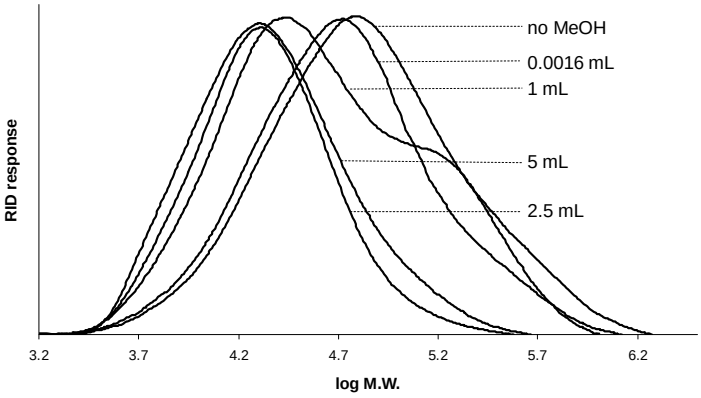

Figure 12. SEC-trace of polymers obtained from the reaction of **6** and EDA in mixtures of chloroform and methanol (the signals were normalized).

This is a first indication (see also section 6.2.4) that even the polymer producing species formed from **6** consists of a mixture of at least two different active species. It seems that methanol has a profoundly different influence on the relative propagation versus termination rates of these species.

In the next experiments, $[\{Rh^{I}(1,5\text{-cyclooctadiene})(\mu\text{-Cl})\}]_2$ was used for the polymerization reactions. This dimer can break up relatively easy and possibly form the active species in the presence of alcohols. The polymerization reactions were performed in the presence of different alcohols; methanol, ethanol and butanol. The amount of 1 mL of alcohol was chosen, because this resulted in the most significant effect with catalyst precursor **6** (Table 4).

Table 5. Polymerization of EDA with $[\{Rh^{I}(1,5\text{-cyclooctadiene})(\mu\text{-Cl})\}]_2$ in DCM/alcohol mixtures.[a]

entry	alcohol	polymer yield (%)[b]	M_w (kDa)[b,c]	M_w/M_n[b,c]	IE (%)[d]
1	-	20	135	2.2	1.4
2	methanol	15	20	1.6	6.9
3	ethanol	20	25	1.9	5.9
4	butanol	25	30	2.0	6.3

[a] Conditions: 0.02 mmol pre-catalyst, 2 mmol of EDA, 5 mL of dichloromethane, 1 mL of alcohol, room temperature, reaction time: 14 hours. [b] Isolated by precipitation and washing with MeOH. [c] SEC analysis calibrated against polystyrene samples.[d] Initiation efficiency: number of polymer chains per Rh in % (mol/mol × 100%).

The polymerization reaction with $[\{Rh^{I}(1,5\text{-cyclooctadiene})(\mu\text{-Cl})\}]_2$ affords polymers in lower yields compared to the reaction with **6** (entry 1 in Table 5). While the polymer yields obtained in the presence of methanol, ethanol and butanol do not improve much compared to the reaction in pure dichloromethane, the initiation efficiencies are significantly higher, leading to shorter polymers (entries 2-4). The molecular weights of the polymers are substantially lowered (~ 25 kDa) with polydispersities of approximately 2.

This could well mean that alcohols are functioning as chain-transfer agents for the small amount of active species responsible for the stereoregular polymerization activity. On the other hand, the alcohols may also generate more active species. In fact, the effect of the alcohols is somewhat larger than reflected in Table 5, because the molecular weight distribution is such that a small part of the formed stereoregular polymer has a too low molecular weight to precipitate from methanol during work-up. This is clear from ^{1}H NMR spectroscopy analysis of the methanol soluble oligomeric fraction, which clearly shows the presence of the short stereoregular polymer (the backbone signal at δ 3.1 ppm in Figure 13) in the mixture containing mostly the atactic oligomers described in Chapter 2.

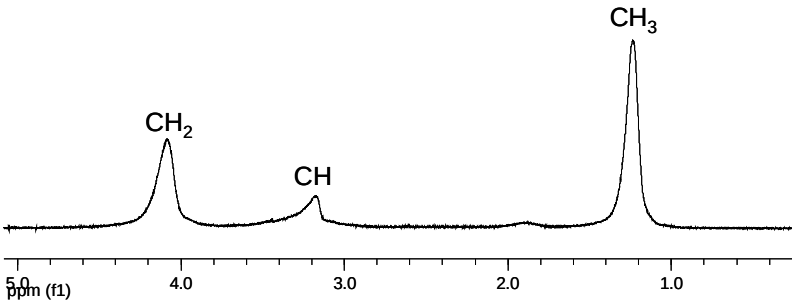

Figure 13. ^{1}H NMR spectrum of methanol soluble fraction of the polymerization of EDA in the presence of methanol (300 MHz, RT, $CDCl_3$).

Analysis of these methanol soluble fractions with MALDI-ToF MS afforded the spectra shown in Figure 14, which reveal very clear repeating patterns with mass differences of 86 Da (corresponding with the mass of CHCOOEt). The series are much clearer than those obtained from the atactic oligomeric mixtures described in section 6.2.2 for which in most cases multiple repeating patterns are observed and which show weak signal to noise ratios. The much clearer patterns observed in Figure 14 for the oligomers prepared in the presence of alcohols are therefore likely dominated by the well-defined stereoregular fraction (as also detected by NMR spectroscopy).

The series of the oligomers prepared in the presence of ethanol and butanol appear at 14 Da and 42 Da higher masses than those prepared in methanol. These differences are the same as the mass differences between the alcohols and the series clearly correspond to oligomers with –H and –alkoxy end-groups and all have sodium as a charge carrier: $[Na]^{+}\{(H–(CHCOOEt)_n–OR)\}$, with R = Me, Et or Bu (see Figure 15).

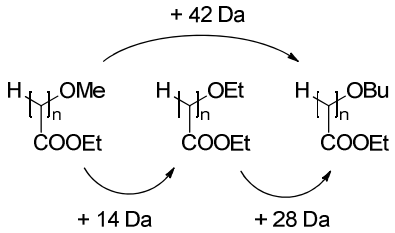

Figure 15. Oligomer fragments observed in MALDI-ToF mass spectra of oligomers obtained with [{Rh^{I}(1,5-cyclooctadiene)(μ-Cl)}]$_2$ in the presence of methanol, ethanol or butanol.

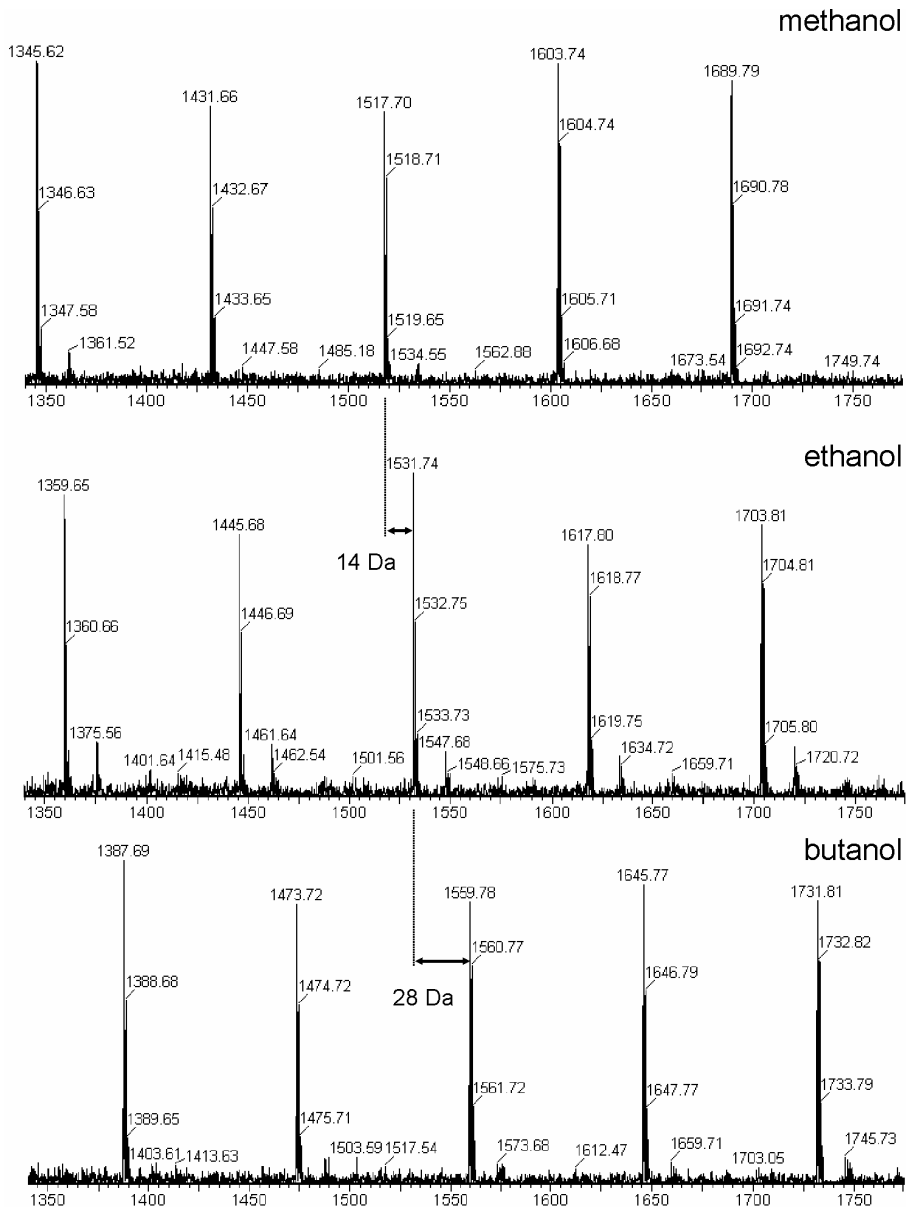

Figure 14. Part of the MALDI-ToF mass spectra (reflectron mode) of oligomers obtained with [{Rh^{I}(1,5-cyclooctadiene)(μ-Cl)}]$_2$ in the presence of methanol, ethanol or butanol.

Although the polymers prepared in the presence of methanol have lower molecular weights, the analysis by MALDI-ToF mass spectrometry is still difficult. For this technique the mass of a polymer should not exceed 10,000 Da. However, in the linear mode a spectrum was obtained and a part of it is shown in Figure 16. The repeating unit is again 86 Da and the residual mass of the peaks observed is 55 Da, again corresponding with: $[Na]^+\{(H-(CHCOOEt)_n-OMe)\}$.

Figure 16. Part of the MALDI-ToF mass spectra (linear mode) of polymer obtained with $[\{Rh^I(1,5\text{-cyclooctadiene})(\mu\text{-Cl})\}]_2$ in the presence of methanol.

On the basis of the previous observations, we propose the mechanism depicted in Figure 17 to explain the formation of $H-(CHE)_n-OR$ oligomers and polymers, as well as the increased average amount of chains per added Rh (initiation efficiency). The latter effect can be explained by the presence of the alcohols causing an increased amount of active Rh-species, or by the alcohols functioning as a chain-transfer agent, or a combination of these effects. Both effects are covered in the mechanism shown in Figure 17.

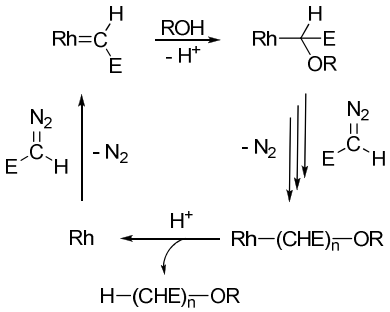

Figure 17. Proposed chain-initiation and chain-transfer mechanisms for carbene polymerization in the presence of alcohols.

Alcohol attack at a non-chain bearing Rh-carbene unit can lead to a Rh–C bond in order to initiate chain growth, and the combination of the reactions shown in Figure 17 provide a plausible chain-transfer mechanism in the presence of alcohols.

6.2.4 The influence of side-product formation and dilution on the performance of the catalyst

In this last part the influence of the dimeric side products on the polymerization reaction is studied. Most of the diethyl fumarate (DEF) and maleate (DEM) is formed in the beginning of the reaction, directly after mixing catalyst precursor **6** with EDA (see Chapter 4).[3] To evaluate their effect one of the dimers or a mixture of both was added to a solution of **6** in chloroform before EDA was added (Table 6).

Table 6. Polymerization of EDA with **6** in the presence of dimers.[a]

entry	diethyl maleate (mmol)	diethyl fumarate (mmol)	isolated polymer yield (%)[b]	M_w (kDa)[c]	M_w/M_n[c]
1	-	-	45	150	3.6
2	2	-	23	98	3.3
3	-	2	18	74	2.8
4	1	1	26	129	3.7

[a] Conditions: 0.04 mmol catalyst; 2 mmol EDA, 5 mL chloroform (solvent), room temperature, reaction time: 14 hours. [b] Isolated by precipitation and washing with MeOH. [c] SEC analysis calibrated against polystyrene samples.

Clearly, there is a negative effect of the presence of DEM and DEF on the polymerization activity of **6**; the yields drop from ~50% to ~ 20% and the molecular weights are also lower (entries 2-4). The formation of dimers was suppressed previously by 'aging' catalyst precursor **10** in air (Chapter 5).[5] However, catalyst precursor **6** does not show this behavior and therefore a different approach was used. To decrease the influence of the presence of the dimers during the polymerization reaction, the reaction mixture was diluted. The experiments were all performed in a similar way with increasing amounts of solvents (Table 7).

Table 7. Polymerization of EDA with **6** at different catalyst and substrate concentrations.[a]

entry	solvent (mL)	polymer yield (%)[b]	M_w (kDa)[b,c]	M_w/M_n[b,c]	oligomer yield (%)[d]
1	5	42	126	3.3	34
2	15	52	161	4.0	32
3	25	65	160	3.7	28
4	35	58	178	4.4	28
5	45	57	167	4.3	30
6	70	58	174	4.7	31
7	100	44	180	4.9	25
8	200	40	180	5.1	42

[a] Conditions: 0.04 mmol catalyst; 2 mmol EDA, solvent: chloroform, room temperature, reaction time: 14 hours. [b] Isolated by precipitation and washing with MeOH. [c] SEC analysis calibrated against polystyrene samples.[d] MeOH soluble fractions after evaporation of the solvent.

The results improve upon dilution of the reaction mixture; the highest polymer yields (approximately 60%, entries 3-6) are obtained in 25-70 mL of chloroform. The molecular weights increase to 180 kDa for the reactions in 100 or 200 mL of chloroform (entries 7 and 8).

Remarkably, the polydispersities increase from ~3 in 5 mL of solvent to ~5 in 200 mL. In the SEC-trace of the polymer samples this becomes clear by the observation of a bimodal polymer distribution (Figure 18).

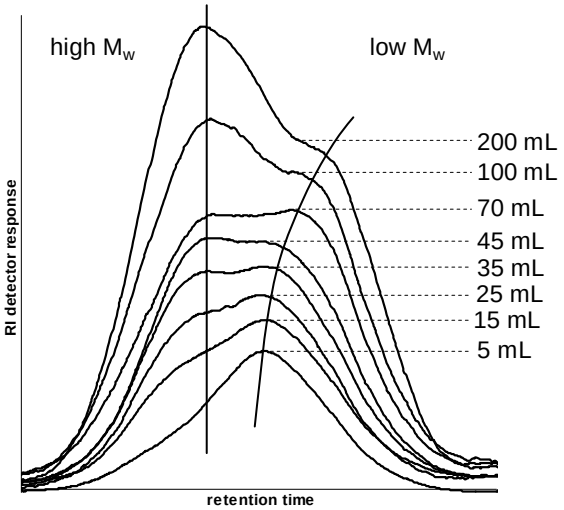

Figure 18. SEC-traces of polymer samples obtained in diluted reaction mixtures of precatalyst **6** and EDA in chloroform (the peak intensities were adjusted to obtain a clear picture).

While the reaction performed in 5 mL of chloroform shows one broad signal, the polymers prepared in the more diluted reaction mixtures show a bimodal distribution with two overlapping signals (Figure 18). This observation points to the presence of two active polymer forming species. The higher molecular weight signals (at the left in Figure 18) seem to retain their position in the chromatogram independent of the concentration. The lower molecular weight fraction shift to even lower weights when the reaction mixture becomes more diluted. It seems that at higher concentrations the reaction is dominated by an active species producing somewhat lower M_w polymers, for which the reactions have a clear order in the [EDA] concentration. For that reason the molecular weights drop upon diluting the reaction mixture. Upon further dilution the reaction becomes dominated by the activity of another active Rh species. The reactions catalyzed by this second species apparently have no, or at least a much lower order in the [EDA] concentration. This explains why the second species takes over the activity upon diluting, as well as the fact that the M_w of the polymer produced by this second species is hardly influenced upon diluting the reaction mixture.

To investigate if chain-transfer occurs under these diluted conditions, the reaction in 45 mL of chloroform was monitored in time (Table 8). Remarkably, already within 10 minutes high molecular-weight polymers are formed in moderate yield. Chain propagation is apparently much faster under these diluted conditions than at higher concentrations (see Chapter 4). The polymer yield increases to 57% at the end of the reaction (Table 7, entry 5), while the molecular weight does not increase significantly in time. The SEC-traces of these experiments are shown in Figure 19. These data point to *slow initiation* and/or *chain-transfer* but *fast propagation* occuring under the applied diluted conditions.

Table 8. Polymerization of EDA with **6** in a diluted reaction mixture (45 mL) at different times.[a]

entry	time (min)	polymer yield (%)[b]	M_w (kDa)[b,c]	M_w/M_n[b,c]	oligomer yield (%)[d]
1	10	17	169	4.0	23
2	25	22	167	4.0	26
3	40	25	176	4.0	24
4	55	27	181	3.7	24

[a] Conditions: 0.04 mmol of catalyst; 2 mmol of EDA, 45 mL of chloroform, room temperature, reaction time: 14 hours. [b] Isolated by precipitation and washing with MeOH. [c] SEC analysis calibrated against polystyrene samples.[d] MeOH soluble fractions after evaporation of the solvent.

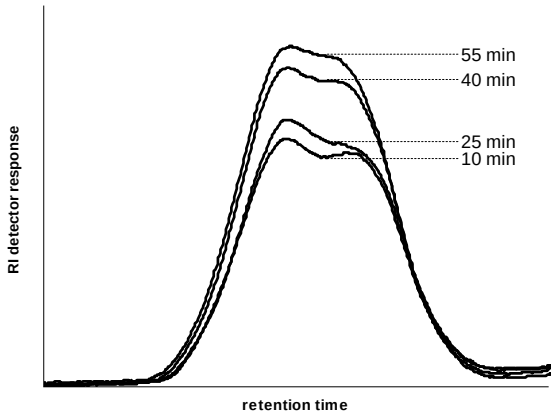

Figure 19. SEC-traces of polymer samples obtained in a diluted reaction mixture (45 mL) of **6** and EDA in chloroform at different reaction times (the peak intensities were adjusted to obtain a clear picture)

The above results obtained under diluted conditions (45 mL of solvent) differ markedly from the data gathered previously at higher concentrations (5 mL of solvent). Monitoring the reaction with EDA at higher concentrations (5 mL of solvent) clearly allowed us to observe the chain-growth process in time (see Chapter 4).[3] Under these conditions the polymerization characteristics allowed us to prepare block copolymers using two different diazoesters (see Chapter 7). Apparently at higher concentrations both the chain-growth and chain termination processes are

slow, likely by competing active site occupation (*e.g.* competing equilibria involving nitrogen or oxygen bound EDA). The chain growth and chain termination process are both faster under more dilute conditions using 45 mL of solvent, thus explaining the observed increasing yields of the same polymer in time without significant changes in the polymer M_w and PDI values.

The increasing polymer yields in time *without formation of higher molecular weight polymers* observed under these dilute conditions can only be explained in two ways (or a combination of these):

(a) Under diluted conditions the initiation/activation process is slowed down, and gradually over time active polymer forming Rh species are being generated which propagate and terminate relatively fast under the applied diluted conditions.

(b) Under the applied diluted conditions (45 mL of solvent) chain-transfer occurs at a competing rate, so that each *active* polymer forming Rh site produces more than one polymer chain. At higher concentrations (5 mL of solvent) chain-transfer is suppressed and plays a minor role within the time frame of the experiment.

We are currently unable to distinguish between these possibilities. A slowed down initation/activation process at lower concentrations is perhaps the most logical explanation considering the results obtained in section 6.2.2 (Figure 11), suggesting that modification of the Rh(diene) precatalyst by EDA changes its activity from dimerization to atactic oligomerization and finally stereoregular polymerization.

6.3 Conclusions

The results described in this Chapter provide valuable information about catalysts activation, chain initiation, chain termination and chain-transfer processes occurring during Rh-mediated carbene polymerization reactions. The use of well defined (diene)Rh^{I}-alkyl/aryl complexes does not lead to better initiation efficiencies, and hence catalyst activation under the applied reaction condition seems to be an important factor for the formation of high molecular-weight and stereoregular polycarbenes.

The combined experiments reveal a complex picture of the polymerization reaction; at least four different species are operative: one for the dimerization, one for the oligomerization and two for the polymerization reaction. It seems that the chains start to grow from (diene)Rh–Y species (Y = anionic nucleophile or nucleophilic ligand), which undergo rapid β-hydrogen elimination in their non-modified forms, thus effectively leading to dimerization activity. Modification of these (diene)Rh–Y and (diene)Rh–H species under the applied reaction conditions leads to species for which β-hydrogen elimination is absent or suppressed, thus leading to the formation of atactic oligomers. Further catalyst modification then allows the formation of stereoregular polymers. MALDI-ToF mass spectrometry analysis of the oligomers reveals the presence of saturated H–$(CHCOOEt)_n$–H and

Y–$(CHCOOEt)_n$–H chains, suggesting that termination involves protonolysis in all cases. Chain-transfer takes place under the influence of alcohols (when added in high concentrations). Under such chain-transfer conditions RO–$(CHCOOEt)_n$–H chains (R= Me, Et, Bu) are formed exclusively. The presence of the DEF and DEM dimeric products negatively influences the polymerization, and leads to lower polymer yields when they are added deliberately.

6.4 Experimental

General procedures

All manipulations, except the work-up of polymerization reactions, were performed under an argon atmosphere using standard Schlenk techniques. Methanol and dichloromethane distilled from calcium hydride and toluene distilled from sodium and tetrahydrofuran, diethyl ether and pentane distilled from sodium benzophenone ketyl under nitrogen were used for metal complex synthesis. Chloroform (stabilized by ethanol; 0.5-1.5 %w/v) was purchased from Biosolve and used as such. The syntheses and catalytic activity of $[\{Rh^I(1,5\text{-cyclooctadiene})(\mu\text{-OAc})\}]_2$[14] (**11**), $[(L\text{-prolinate})Rh^I(1,5\text{-cyclooctadiene})]$[2,3] (**6**), $[(L\text{-prolinate})Rh^I(1,5\text{-dimethyl-1,5-cyclooctadiene})]$[5] (**10**), $[(\text{glycinate})Rh^I(1,5\text{-cyclooctadiene})]$[3] (**12**), $[(L\text{-prolinate})Rh^I(2,5\text{-norbornadiene})]$[3] (**8**), $[(L\text{-prolinate})Rh^I(\textit{endo}\text{-dicyclopentadiene})]$[3] (**7**), $[(L\text{-prolinate})Rh^I(1,5\text{-hexadiene})]$ (**9**) (Chapter 4) have been described previously. HBArF,[10] $[\{Rh^I(1,5\text{-cyclooctadiene})(\mu\text{-Cl})\}]_2$,[15] $[\{Rh^I(1,5\text{-cyclooctadiene})(\mu\text{-Me})\}]_2$[11] (**1**), $[\{Rh^I(1,5\text{-cyclooctadiene})(L)(Me)\}]$ (**2**, L = pyridine),[12] $[(1,5\text{-cyclooctadiene})Rh(\mu\text{-}CH_2\text{-py-6Me-}C,N)]_2$[8] (**3**) and $[(TACN)Rh(Me)_3]$[9] (**5**) were prepared according to published procedures. All other chemicals were purchased from commercial suppliers and used without further purification. NMR spectroscopy experiments were carried out on a Varian Inova 500 spectrometer (500 MHz and 125 MHz for ^1H and ^{13}C, respectively) or a Varian Mercury 300 spectrometer (300 MHz, 121.5 MHz and 75 MHz for ^1H, ^{31}P and ^{13}C, respectively). Assignment of the signals was aided by COSY, ^{13}C HSQC and APT experiments. Solvent shift reference for ^1H NMR spectroscopy: $CDCl_3$: δ_H = 7.26 ppm. For ^{13}C NMR spectroscopy: $CDCl_3$: δ_C = 77.0 ppm. Abbreviations used are: s = singlet, d = doublet, dd = doublet of doublets, m = multiplet, cod = 1,5-cyclooctadiene, dcp = *endo*-dicyclopentadiene, pro = prolinate. IR solid state measurements were performed on a Shimadzu FTIR 8400S spectrometer equipped with a Specac MKII Golden Gate Single Reflection ATR system. Elemental analyses (CHN) were performed by the Kolbe analytical laboratory in Mülheim an der Ruhr (Germany). Molecular-weight distributions were measured using size-exclusion chromatography (SEC) on a Shimadzu LC-20AD system with two PLgel 5µm MIXED-C columns 300 mm x 7.5 mm (Polymer Laboratories) in series (1 mL/min and T = 35°C) or with Waters Styragel HR1, HR2, and HR4 (300 mm x 7.8 mm) columns in series (1 mL/min and T = 40°C) and a Shimadzu RID-10A refractive-index detector, using dichloromethane as mobile phase. Polystyrene standards in the range of 760-1,880,000 g/mol (Aldrich) were used for calibration.

Synthesis of [(mesityl)Rh^{I}(1,5-cyclooctadiene)(triphenylphosphine] (4)[16]

[Mes]Li was prepared by addition of *n*-butyllithium (0.4 mL; 1 mmol of a 2.5 M solution in hexanes) to a cooled (–50°C) solution of 2-bromomesitylene (0.15 mL; 200 mg; 1 mmol) in tetrahydrofuran (5 mL). The solution was stirred for 10 minutes and subsequently warmed to room temperature. A yellow solution of [{Rh^{I}(1,5-cyclooctadiene)(μ-Cl)}]$_2$ (123 mg; 0.25 mmol) and triphenylphosphine (295 mg; 1.13 mmol) in tetrahydrofuran (10 mL) was added to the [Mes]Li solution at room temperature. After stirring the obtained orange solution for 30 minutes, methanol (2 mL) was added. The solvent was removed *in vacuo* and the product was purified by column chromatography (aliminium oxide 90 active neutral (Merck), toluene). The yellow fraction was collected and the solvent was evaporated. Washing with pentane (3× ~1 mL) and drying *in vacuo* afforded an orange solid (110 mg; 37%). Cooling (–20°C) a solution of **4** in *n*-hexane yielded crystals suitable for X-ray diffraction.
^{1}H NMR (500 MHz, $CDCl_3$, 298 K): δ 7.34-7.28 and 7.24-7.18 (m, 15H, PPh_3), 6.38 (s, 2H, CH_{Mes}), 4.66 (m, 2H, CH=CH), 3.67 (m, 2H, CH=CH), 2.5-2.3 (m, 4H, CH_2–cod), 2.37 (s, 6H, *o*-Me), 2.2-2.1 (m, 2H, CH_2–cod), 2.1-2.0 (m, 2H, CH_2–cod), 2.12 (s, 3H, *p*–Me) ppm. ^{13}C NMR (125 MHz, $CDCl_3$, 298 K): δ 142.54 (d, J = 2 Hz, C_q), 134.10 (d, J_{C-P} = 11 Hz, PPh_3–CH) 133.96 (s, C_q), 133.68 (s, C_q), 131.10 (s, C_q), 129.02 (d, J_{C-P} = 2 Hz, PPh_3–*p*–CH), 127.50 (d, J_{C-P} = 9 Hz, PPh_3–CH), 126.22 (s, Mes–CH), 93.67 (dd, $^{1}J_{C-Rh}$ = 10 Hz, $^{2}J_{C-P}$ = 10 Hz, CH=CH *trans* to PPh_3), 86.12 (d, $^{1}J_{C-Rh}$ = 7 Hz, CH=CH *trans* to Mes), 31.01 (s, cod–CH_2), 30.51 (d, $^{3}J_{C-P}$ = 2 Hz, cod–CH_2), 26.04 (s, CH_3), 20.58 (s, CH_3) ppm. ^{31}P NMR (121 MHz, $CDCl_3$, 298 K): δ 25.70 (d, $^{1}J_{P-Rh}$ = 181 Hz) ppm. Elemental analysis for $C_{35}H_{38}PRh$: calcd. C 70.94, H 6.46; found C 71.27, H 6.29%. Summary of the crystal data for: **4**, $C_{35}H_{38}PRh$, M_r = 592.53, crystal size = 0.27 x 0.15 x 0.08 mm, monoclinic, space group: *C2/c*, a = 32.151(4) Å, b = 9.3724(10) Å, c = 19.869(3) Å, β = 107.394(9)°, V = 5713.5(13) Å^3, Z = 8, ρ_{calcd} = 1.378 g cm^{-3}, F(000) = 2464, μ(MoKα) = 6.76 cm^{-1}, T = 208(2) K, λ(MoKα) = 0.71073 Å, θ range = 2.15 to 27.50°, reflections collected = 84976, unique = 6567 (R_{int} = 0.0551), final R indices [I>2σ(I)] = R_1 = 0.0403, wR_2 = 0.0905, R indices (all data) = R_1 = 0.0502, wR_2 = 0.0940.

Polymerization of carbenes from ethyl diazoacetate

Standard experiment. Ethyl diazoacetate (EDA) (2 mmol) was added to a yellow solution of catalyst precursor (0.04 mmol) in chloroform (5 mL). Upon addition, gas evolution was visible, and the color of the reaction mixture became slightly darker. The mixture was stirred for 14 h at room temperature. Subsequently the solvent was removed *in vacuo*, and methanol was added to the oily residue. The precipitate was centrifuged and washed with methanol until the washings were colorless. The resulting white powder was dried *in vacuo* and identified as poly(ethyl 2-ylidene-acetate) (PEA) using ^{1}H NMR spectroscopy. For the dilution experiments larger amounts of chloroform were used. Some experiments were performed in the presence of additives, such as methanol, diethyl fumarate and maleate (see main text).
With catalyst precursor **1**.[11] A suspension of [{Rh^{I}(1,5-cyclooctadiene)(μ-Cl)}]$_2$ (39 mg; 0.08 mmol) in diethyl ether was cooled to –70°C. Methyl lithium (0.1 mL; 0.16 mmol; 1.6 M

in Et_2O) was added and the obtained orange solution was stirred for 1 h at −70°C. The clear orange solution was warmed to −40°C and EDA (3.9 g; 32 mmol) was added. The color of the reaction mixture became darker and then yellow. No gas evolution was observed at this point. The reaction vessel was placed in an ice bath and stirred for 2 h, during which gas evolved and the color of the reaction mixture turned orange. After 45 min at 0°C the mixture became turbid. The reaction mixture was stored overnight at 4°C. After warming to room temperature, a white precipitate was visible in the orange solution. The solid product was filtered and washed with diethyl ether and dried *in vacuo*. Yield: 0.08 g; 3%.

With catalyst precursor **2**. Complex **2** was prepared according to published procedures[12] (from: $[\{Rh^{I}(1,5\text{-cyclooctadiene})(\mu\text{-Cl})\}]_2$ (20 mg; 0.04 mmol), methyl lithium (0.05 mL; 0.08 mmol; 1.6 M in diethyl ether) and pyridine (0.01 mL; 0.1 mmol) in diethyl ether (20 mL)) and was not isolated before reaction with EDA. EDA (0.9 g; 8 mmol) in dichloromethane (10 mL) was added to the reaction mixture of the synthesis of **2**. The color of the solution changed from yellow to orange. After stirring for 14 h at room temperature the solvent was removed *in vacuo* and methanol was added to the oily residue. The precipitate was centrifuged and washed with methanol until the washings were colorless. The resulting white powder was dried *in vacuo*. Yield: 40 mg; 6%.

With catalyst precursors **3** *and* **4**. Ethyl diazoacetate (EDA) (**3**: 210 mg, 1.84 mmol; **4**: 244 mg, 2 mmol or 1.22 g, 10 mmol, respectively) was added to a solution of catalyst (**3**: 7 mg, 0.01 mmol; **4**: 24 mg, 0.04 mmol or 12 mg, 0.02 mmol, respectively) in chloroform (**4**: 5 or 25 mL, respectively) or dichloromethane (**3**: 5 mL). The mixture was stirred for 14 hours at room temperature. Subsequently the solvent was removed *in vacuo* and methanol was added to the oily residue. The precipitate was centrifuged and washed with methanol until the washings were colorless. The resulting white powder was dried *in vacuo*.

With complex **5**. EDA (0.5 mL) was added to a solution of **5** (0.02 g; 0.04 mmol) in dichloromethane (5 mL) at room temperature. The reaction mixture was stirred for 2 h during which no gas evolution was observed. Subsequently, $HBArF$[10] (64 mg; 0.07 mmol) was added. Analysis by ^1H NMR showed that no reaction occurred.

With $[\{Rh^{I}(1,5\text{-cyclooctadiene})(\mu\text{-Cl})\}]_2$. Ethyl diazoacetate (EDA) (2 mmol) was added to a yellow solution of catalyst precursor (0.02 mmol) in dichloromethane (5 mL) with or without an alcohol (1 mL). The mixture was stirred for 14 h at room temperature. Subsequently the solvent was removed *in vacuo*, and methanol was added to the oily residue. The precipitate was centrifuged and washed with methanol until the washings were colorless. The resulting white powder was dried *in vacuo*.

MALDI-ToF mass spectrometry. Oligomers prepared with precatalysts **6**, **11** and **12** were filtered through a silica plug before analysis. The mass spectra shown in Figures 7-10 and 16 were recorded using a Kratos Axima-CFR MALDI-ToF mass spectrometer (Kratos Analytical LTD., Manchester, England), equipped with a nitrogen laser (λ = 337 nm), operating with a pulse repetition rate of 10 Hz. In linear mode positive ion spectra were recorded, accumulating 100 acquisitions. In reflectron mode, 173 lasershots were accumulated. Ions were accelerated at 20 kV, applying a pulsed extraction delay time optimized for higher masses (> 13000 Da). The instrument was externally calibrated, using three standard peptide solutions in the mass range 12,000 to 60,000 Da. For these solutions a maximum deviation of 1 mDa of the true mass was found. 2-(4-Hydroxyphenylazo)benzoic

acid (HABA) was used as a matrix. The matrix (20 mg/mL) and the oligomer (7 mg/mL) were dissolved in THF and the polymer (7 mg/mL) in chloroform. The measurements were performed with and without the addition of salts (potassium-, lithium- and silver trifluoroacetate). The spectra in Figure 14 were recorded on a Tofspec 2EC mass spectrometer (Micromass, Wythenshawe, U.K.) provided with a 2 GHz digitizer. For reflectron MALDI-ToF MS, 0.5 μL of oligomer solution (7 mg/mL) was mixed with 0.5 μL of HABA (20 mg/ml) in THF was spotted on a MALDI target plate and dried.

6.5 Acknowledgements

Annemarie Walters is acknowledged for her contributions to this Chapter. Petra Aarnoutse and Henk Dekker are thanked for MALDI-ToF mass spectrometry analysis of the oligomers and polymers. Jan Smits (RU Nijmegen) is thanked for the X-ray structure determination.

6.6 References

1 Jellema, E.; Jongerius, A. L.; Reek, J. N. H.; de Bruin, B. *Chem. Soc. Rev.* **2010**, *39*, 1706.
2 Hetterscheid, D. G. H.; Hendriksen, C.; Dzik, W. I.; Smits, J. M. M.; van Eck, E. R. H.; Rowan, A. E.; Busico, V.; Vacatello, M.; Van Axel Castelli, V.; Segre, A.; Jellema, E.; Bloemberg, T. G.; de Bruin, B. *J. Am. Chem. Soc.* **2006**, *128*, 9746.
3 Jellema, E.; Budzelaar, P. H. M.; Reek, J. N. H.; de Bruin, B. *J. Am. Chem. Soc.* **2007**, *129*, 11631.
4 Rubio, M.; Jellema, E.; Siegler, M. A.; Spek, A. L.; Reek, J. N. H.; de Bruin, B. *Dalton Trans.* **2009**, 8970.
5 Jellema, E.; Jongerius, A. L.; Walters, A. J. C.; Smits, J. M. M.; Reek, J. N. H.; de Bruin, B. *Organometallics* **2010**, *29*, 2823.
6 a) Yamamoto, M.; Onitsuka, K.; Takahashi, S. *Organometallics* **2000**, *19*, 4669. b) Saeed, I.; Shiotsuki, M.; Masuda, T. *Macromolecules* **2006**, *39*, 8567. c) Saeed, I.; Shiotsuki, M.; Masuda, T. *Macromolecules* **2006**, *39*, 8977.
7 Lahoz, F. J.; Martin, E.; Tiburcio, J.; Torrens, H.; Terreros, P. *Transition Met. Chem.* **1994**, *19*, 381.
8 Chebi, D. E.; Fanwick, P. E.; Rothwell, I. P. *Organometallics* **1990**, *9*, 2948.
9 Wang, L.; Flood, T. C. *J. Am. Chem. Soc.* **1992**, *114*, 3169.
10 Brookhart, M.; Grant, B.; Volpe Jr, A. F. *Organometallics* **1992**, *11*, 3920.
11 Schmidt, G. F.; Muetterties, E. L.; Beno, M. A.; Williams, J. M. *Proc. Natl. Acad. Sci. U. S. A.* **1981**, *78*, 1318.
12 Kulzick, M. A.; Price, R. T.; Andersen, R. A.; Muetterties, E. L. *J. Organomet. Chem.* **1987**, *333*, 105.
13 See for example: Bonge, H. T.; Pintea, B.; Hansen, T. *Org. Biomol. Chem.* **2008**, *6*, 3670.
14 Sheldrick, W. S.; Günther, B. *J. Organomet. Chem.* **1989**, *375*, 233.
15 Giordano, G.; Crabtree, R. H. *Inorg. Synth.* **1990**, *28*, 88.
16 Similar to published procedures: Miyake, M.; Misumi, Y.; Masuda, T. *Macromolecules* **2000**, *33*, 6636.